frontiers in Chemistry

ORIGINAL RESEARCH
published: 05 November 2021
doi: 10.3389/fchem.2021.782238

Starch-Based Carbon Dots for Nitrite and Sulfite Detection

Panyong Wang[1], Yan Zhang[2], Yulu Liu[1,3], Xinpei Pang[1,3], Pai Liu[3], Wen-Fei Dong[3,4], Qian Mei[3,4], Qing Qian[3], Li Li[3]* and Ruhong Yan[2]**

[1]School of Biomedical Engineering (Suzhou), Division of Life Sciences and Medicine, University of Science and Technology of China, Hefei, China, [2]The Affiliated Suzhou Science and Technology Town Hospital of Nanjing Medical University, Suzhou, China, [3]CAS Key Laboratory of Biomedical Diagnostics, Suzhou Institute of Biomedical Engineering and Technology, Chinese Academy of Science (CAS), Suzhou, China, [4]Jinan Guokeyigong Science and Technology Development Co., Ltd, Jinan, China

Nitrite and sulfite play important roles in human health and environmental science, so it is desired to develop a facile and efficient method to evaluate NO_2^- and SO_3^{2-} concentrations. In this article, the use of green alternatives with the potential of multi-functionality has been synthesized to detect nitrite and sulfite based on fluorescent probe. The carbon dots (CDs) with starch as only raw materials show fluorescence turn "on-off-on" response towards NO_2^- and SO_3^{2-} with the limits of detection of 0.425 and 0.243 μM, respectively. Once nitrite was present in the solution, the fluorescence of CDs was quenched rapidly due to the charge transfer. When sulfite was introduced, the quenching fluorescence of CDs was effectively recovered because of the redox reaction between NO_2^- and SO_3^{2-}, and thus providing a new way for NO_2^- and SO_3^{2-} detection. Owing to their excellent analytical characteristics and low cytotoxicity, the "on-off-on" sensor was successfully employed for intracellular bioimaging of NO_2^- and SO_3^{2-}.

Keywords: carbon dots, on-off-on, nitrite and sulfite, starch, fluorescence detection

OPEN ACCESS

Edited by:
Xiaomin Li,
Fudan University, China

Reviewed by:
Lei Lei,
China Jiliang University, China
Lei Wang,
Harbin Institute of Technology, China

****Correspondence:***
Ruhong Yan
yrhzl@hotmail.com
Li Li
lil@sibet.ac.cn
Qing Qian
qianqing@sibet.ac.cn

Specialty section:
This article was submitted to Nanoscience, a section of the journal Frontiers in Chemistry

Received: *24 September 2021*
Accepted: *19 October 2021*
Published: *05 November 2021*

Citation:
Wang P, Zhang Y, Liu Y, Pang X, Liu P, Dong W-F, Mei Q, Qian Q, Li L and Yan R (2021) Starch-Based Carbon Dots for Nitrite and Sulfite Detection. Front. Chem. 9:782238. doi: 10.3389/fchem.2021.782238

INTRODUCTION

Nitrogen oxide is one of the primary pollutants from fuel combustion (Boningari and Smirniotis, 2016). The nitrite was thought to be inert end product of endogenous metabolism of nitric oxide (Lundberg et al., 2008). As food additives to inhibit the growth of microorganisms in cured and processed meats, excessive intake of nitrite ions with food or water can seriously endanger human health (Kalaycioglu and Erim, 2019). With potentially carcinogenic effects (Forman et al., 1985), nitrite can oxidize ferrous iron to trivalent iron to cause the formation of methemoglobin and has been listed as a highly toxic substance by The World Health Organization (Cockburn et al., 2013; Zhao W. et al., 2019). In addition, as a toxic air pollutant, sulfur dioxide is the main precursors of acid rain. Inhaled sulfur dioxide could be hydrated to produce it derivatives sulfite and bisulfite. Sulfite is considered as a restricted food additive in various food preservatives and excessive amounts of sulfite in food and drinking water have been major concerns for public health (Zhang et al., 2014; Wang et al., 2021b). It can cause harmful effects on tissue and has been found to be associated with asthma, hypotension, chronic obstructive pulmonary diseases, cardiovascular and gastrointestinal pain (Joseph et al., 2015; Pan, 2019; Asaithambi and Periasamy, 2020; Heaviside et al., 2021). In terms of the United States Food and Drug Administration (USFDA), the limit of sulfite residue in food is 10–100 ppm (Khan and Lively, 2020). Therefore, developing a rapid, highly selective and water-soluble probe to realize the sequential detection of nitrite and sulfite ions is of great importance.

In recent years, several analytical procedures including digital microfluidic platform, ion-exchange chromatography, ion-pair phase HPLC technique and capillary electrophoresis have been developed for the determination of these ions (Zuo and Chen, 2003; Iammarino et al., 2010; Della Betta et al., 2014; Gu et al., 2020; Zhang et al., 2021). However, these methods either require tedious sample preparation procedures, or are difficult to be widely used due to economic factors. Thus, a simple and inexpensive strategy to sense nitrite ions and sulfite ions with favorable sensitivity is highly desirable. There are many researches on sensing based on fluorescent nanocrystals. For example, lanthanide-doped fluoride nanocrystals are used for temperature sensing with ultrahigh relative sensitivity (Wang et al., 2021c; Wang et al., 2021d). However, their application may be hampered by complicated sample preparation procedure and sometimes the need for toxic raw materials. Carbon dots (CDs), on the other hand, can serve as a promising candidate in this field.

CDs, as these carbon-based fluorescent nanoparticles (typically less than 10 nm) has attracted the tremendous interest of researchers because of their unique properties such as low toxicity, excellent photostability, tunable emission spectra, easy surface functionalization, good biocompatibility and facile synthesis (Sun et al., 2006; Langer et al., 2021; Nazri et al., 2021). Because of these excellent properties, CDs have been applied in bioimaging, sensing, photocatalysis and drug delivery (Wang R. et al., 2018; Wang J. et al., 2019; Tosic et al., 2019; Yue et al., 2019; Jin et al., 2021). For instance, Qu et al. have synthesized bifunctional ibuprofen-based carbon dots for simultaneous bioimaging and anti-inflammatory (Qu et al., 2020). Jiao et la. have developed nitrogen-doped carbon dots for the ratiometric detection of sliver ions and glutathione (Jiao et al., 2019). Yarur et al. have demonstrated the synthesis of ratiometric fluorescence carbon dots for the detection of heavy metal ions with high selectivity and sensitivity (Yarur et al., 2019). As for detection nitrite ions in water, Zan et al. have reported green emission CDs for detection of nitrite ions and bioimaging (Zan et al., 2020). Another CDs synthesized by citric acid and amine were used for determining nitrite with a detection limit of 9.6 μg/L (Li et al., 2020). Chemical heteroatoms doping is an effective method to regulate the intrinsic properties of CDs. Jiang et al. have prepared polymer carbon dots doped with nitrogen and phosphorus to detect nitrite ions and the detection limit was as low as 0.55 μM(Jiang et al., 2019). Unlike nitrite sensors, the work of sulfite ions detected by fluorescence probes based on CDs have been rarely reported. The green fluorescence of upconversion nanoparticles was restored in the presence of sulfite or bisulfite and the limit of detection is 0.14 μM(Wang S. et al., 2018). Another method is the introduction of Cr (IV) into CDs and sulfite was successfully detected by the electron-exchange between Cr (IV) and CDs. The fluorescence of CDs was recovered when Cr (IV) was reduced by sulfite with the detection limitation 0.35 μM (Fang et al., 2017). Although fluorescent probes based on carbon dots have been developed to detect nitrite ions or sulfite ions, there are no reports using carbon dots for the sequential detection of nitrite ions and sulfite ions.

In this paper, we developed a CDs-based probe which can detect NO_2^- and SO_3^{2-} separately through a "on-off-on" mechanism. CDs were prepared using starch as raw material through one-step hydrothermal method, which is simple, environmentally friendly and suitable for large-scale production. The fluorescence intensity was quenched in the presence of nitrite ions and recovered with addition of sulfite derivatives (**Figure 1**). Taking advantage of fast response, stable fluorescence properties and favorable biocompatibility, CDs have been developed for the sensitive detection and imaging of nitrite ions and sulfite ions with the limits of detection of 0.425 and 0.243 μM. In addition, the "on-off-on" detection systems for nitrite ions and sulfite display high sensitivity and selectivity, demonstrating the great potential of CDs in sensing, environmental science and food safety.

MATERIALS AND METHODS

Materials

Starch, L-cysteine (Cys), glycine (Gly), urea, glucose (Glu), calcium chloride ($CaCl_2$), sodium chloride (NaCl), copper chloride ($CuCl_2$), potassium chloride (KCl), iron (III) chloride (FeCl3), glutathione (GSH), sodium sulfate (Na_2SO_4), sodium nitrate ($NaNO_3$), sodium sulfite (Na_2SO_3), sodium phosphate (Na_3PO_4), sodium bisulfite ($NaHSO_4$) and sodium nitrite ($NaNO_2$) were purchased from Sinopharm Chemical Reagent Company (China). Dulbecco's modified Eagle's medium (DMEM) medium and fetal bovine serum (FBS) were purchased from HyClone (United States). WST assay kits were purchased from Energy Chemical (China). All regents were not processed or purified prior to use.

Structure Characterization

Fluorescence spectra were recorded on a fluorescent spectrophotometer (F97Pro, China). UV-vis absorption spectra were recorded on a U-3010 spectrophotometer (Hitachi, Japan). Fluorescence lifetime measurements were carried out on photoluminescence Spectrometer (FLS 1000, United Kingdom). An AXIS ULTRA DLD spectrometer was used to detect X-ray photoelectron spectroscopy (XPS). Freeze dryers (Scientz-10N, CHINA) was used to obtain CDs solid powders. Transmission electron microscopy (TEM, JEOL Ltd, Japan) was used to characterize the morphology of the CDs. Nano ZS/ZEN3690 (Malvern, United Kingdom) was used to investigate the particle size distribution and surface potential of the CDs. Fourier transform infrared (FT-IR) spectra was acquired using an FT-IR spectrometer (Agilent Cary 660, United States).

Synthesis of CDs

The synthesis of CDs was similar to our reported method (Wang et al., 2021a). Typically, 0.5 g starch was dissolved in 30 ml ultrapure water, stirred and ultrasonic vibrated for 10 min, and then heated at 200°C in a 100 ml stainless steel autoclave lined with polytetrafluoroethylene for 10 h. After the solution was cooled to room temperature, centrifuged at 10,000 rpm for 10 min to remove

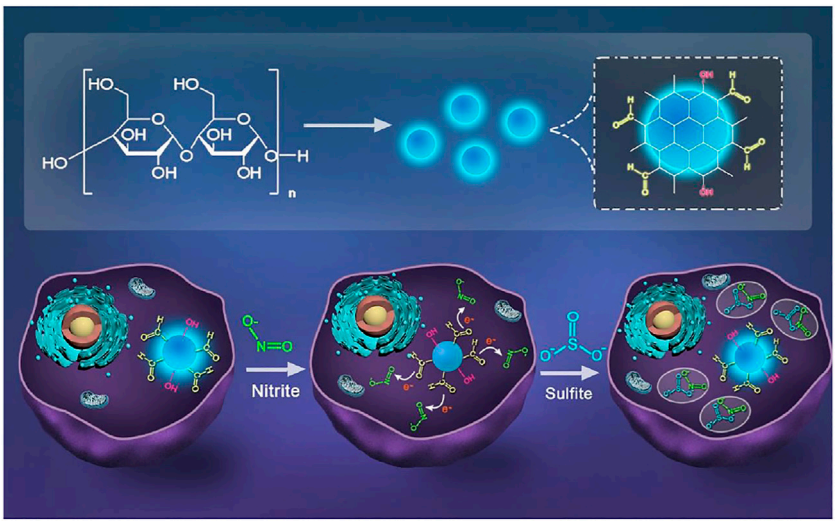

FIGURE 1 | Scheme of synthesizing CDs and schematic illustration for the CDs detection of NO_2^- and SO_3^{2-} in cells.

precipitate, filtered by a 0.22 μm filter membrane to further detach the aggregates and then dialyzed against pure water through a dialysis membrane (M_w = 1,000 Da) for 8 h. The product was lyophilized to obtain dark brown CDs and exhibited strong fluorescence under UV irradiation.

NO_2^- and SO_3^{2-} Fluorescence Assay and Selectivity Studies

To detect of NO_2^-, different concentrations of NO_2^- solutions (10 mM, final concentration 0–700 μM) were added systematically into 3 ml aqueous solutions of CDs (20 μL; the final concentration is 20 μg ml^{-1}), then the sample was oscillated for 5 min at room temperature with a small oscillator at 1,000 rpm. Finally, the emission spectrum of the sample was measured by fluorescence spectrometer at the excitation wavelength of 360 nm. To verify detection selectivity of CDs toward NO_2^-, other ions solutions were examined in a similar way. For the assay of SO_3^{2-}, various concentrations of SO_3^{2-} (10 mM, final concentration 0–700 μM) were obtained by diluting the stock solution with ultrapure water. The subsequent experimental procedure is consistent with the NO_2^- detection process.

Relative Fluorescence Quantum yields

The fluorescence quantum yield is the efficiency of converting absorbed photons into emitted photons (Grabolle et al., 2009). For the unknown sample relative fluorescence quantum yield, we can according to the known absorption and emission of relatively perfect quantum yield standard such as rhodamine 101, quinine sulfate and rhodamine 6G to obtain (Wurth et al., 2013). The QY of CDs was measured using quinine sulfate (55%) as standard (Olmsted, 1979) and was calculated using following equation:

$$QY_s = QY_{st}\,(A_{st}/A_x)\,(I_x/I_{st})\left(\eta_s/\eta_{st}\right)^2$$

Where A_{st} refers to the absorbance of the standard, A_x is the absorbance of the sample to be tested, I represent the emission intensity integral, η represents the refractive index of the solution. The subscript st represents the standard (quinine sulfate), and s represents the sample to be tested (CDs). For more reliable results and to minimize errors, A_s and A_{st} were less than 0.05.

Cytotoxicity Assay

In briefly, HeLa cells were cultured in 0.4% penicillin streptomycin and 10% fetal bovine serum for 24 h in a 5% CO_2 incubator at 37°C, and then the cells were diffused into 96-well plates (100 μL per well, 5,000 cells) and treated with CDs at different concentration (0–500 ug mL^{-1}). After incubation for another 24 h, cytotoxicity of the CDs for HeLa cells was evaluated via a WST assay. The absorbance of each well was measured by a microplate reader at 450 nm after 4 h.

Cell Fluorescence Imaging

HeLa cells were seeded on the coverslips in 6-well plates and incubated at 37°C under 5% CO_2 in DMEM medium containing 10% FBS and 1% penicillin-streptomycin for 24 h. Subsequently, HeLa cells were treated CDs (200 μg ml^{-1}) for a period of 24 h and washed three times with PBS for imaging. For the detection of NO_2^- and SO_3^{2-}, these cells were incubated with 500 μM NO_2^- for 0.5 h. In order to restore the intracellular fluorescence, SO_3^{2-} (500 μM) was added and incubated for another 0.5 h. After washing the cells three times with PBS, the fluorescence images of the samples were observed using a confocal laser microscopy.

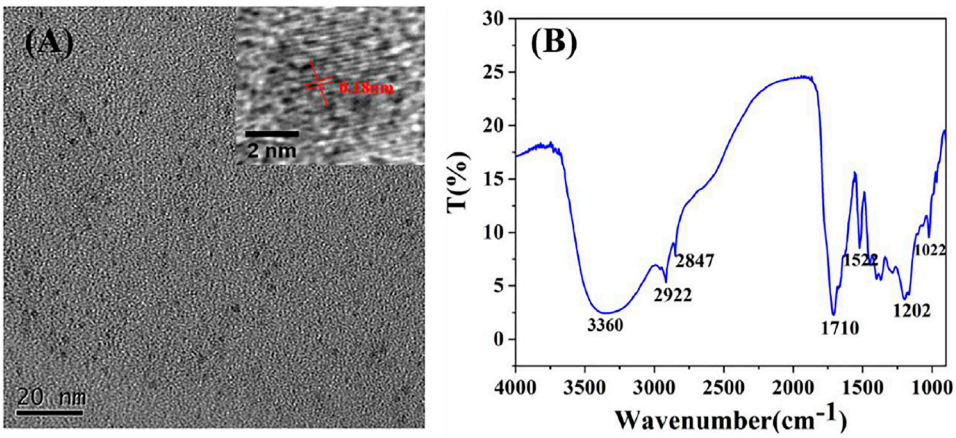

FIGURE 2 | (A) TEM image and HRTEM of CDs **(B)** FT-IR spectrum of CDs sample.

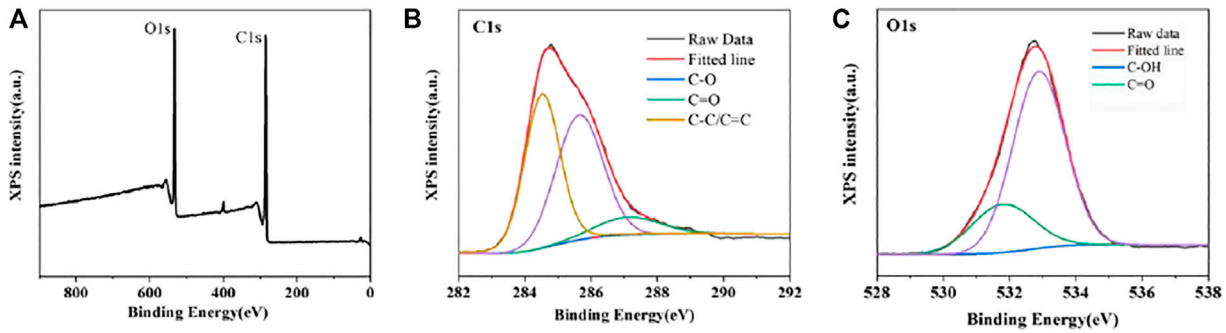

FIGURE 3 | XPS spectra of CDs **(A)** Full-scan spectrum and high-resolution spectrum of C 1s **(B)** and O 1s **(C)**.

RESULTS AND DISCUSSION

The Characterization of CDs

The morphology, surface functional groups, structure and composition of the CDs were investigated by transmission electron microscope (TEM), Fourier transform infrared spectroscopy (FT-IR), Particle size analyzer (ZS nano 90) and X-ray photo-electric spectrometry (XPS). As illustrated in **Figure 2A**, the TEM image and the corresponding histogram of size distribution (**Supplementary Figure S1**) illustrated that CDs with the average particle size of 5.6 nm were uniformly dispersed and spherical shape, indicating they were water-soluble. High resolution TEM image (insert in **Figure 2A**) showed that the particles have a lattice structure and lattice constant is 0.18 nm. In the FT-IR spectrum of the CDs (**Figure 2B**), the broad peak at 3,360 $cm^{-1}$is the telescopic vibration from O-H, the peak at 2,922 cm^{-1} corresponds to the stretching vibration peak of C-H and the peak at 1710 cm^{-1} comes from the stretching vibration of C=O (Ge et al., 2015; Li et al., 2015). The characteristic peak at 1,522 cm^{-1}, 1,202 cm^{-1} and 1,022 cm^{-1} corresponds to the stretching vibration peak of C=C bond, C-C bond and C-OH bond (Zhi et al., 2018), indicating the existence of hydroxyl and various other moieties (such as C-H, C=O and C=C) in the CDs.

Then, XPS was performed to further identify the structural information of CDs. The XPS full scan spectrum in **Figure 3A** contains two distinct peaks at 284.8 (C 1s) and 532.8 eV (O 1s). Further, the major peaks at 284.5, 285.7 and 287.2 eV in the high-resolution C 1s spectrum are respectively the signal peaks of C-C/C=C, C-O and C=O groups. The O 1s XPS spectrum of CDs can be decomposed into peaks at 531.8 and 532.9 eV corresponded to the C=O and C-OH groups. These results further confirm that the presence of carboxyl and hydroxyl functional groups on surface of CDs, which is consistent with the results of the FT-IR spectrum.

To further investigate the optical properties of CDs, UV-vis absorption and fluorescence spectroscopy were also performed. **Figure 4** exhibits an intense absorption peak at 284 nm, which is mainly originated from the π-π transition of C-C bond. Moreover, the maximum fluorescence emission intensity of CDs is located at 435 nm and excitation wavelength at 360 nm. In addition, CDs preserved stable fluorescence in solution with a wide range of pH values from 1 to 10. As demonstrated in **Figure 4**, the fluorescence intensity of CDs

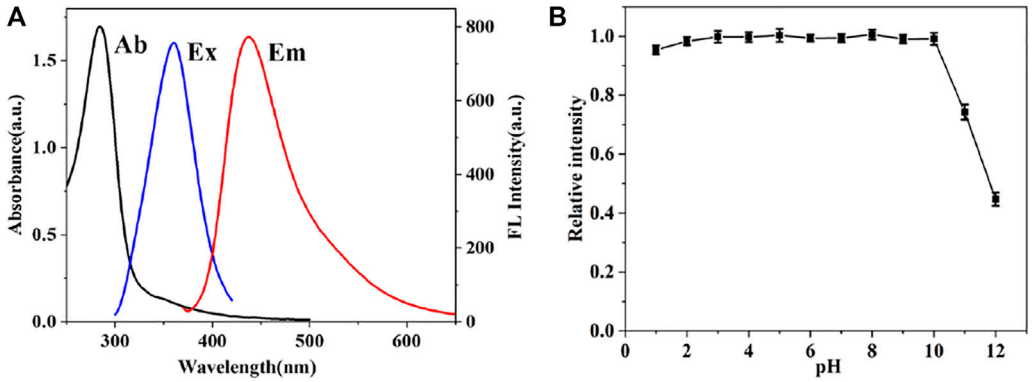

FIGURE 4 | (A) UV-vis absorption spectrum (blank line), fluorescence excitation (blue line) and emission spectra (red line) of CDs **(B)** Influence of the pH on the fluorescence intensity of CDs.

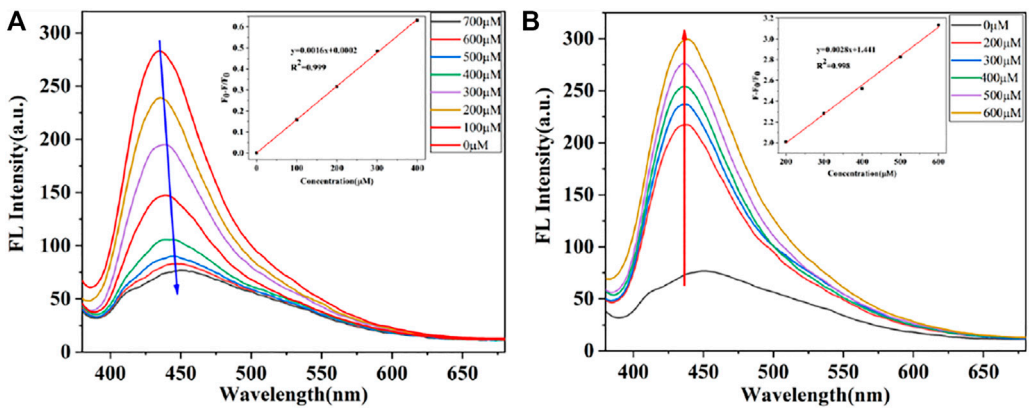

FIGURE 5 | (A) Fluorescence spectra of CDs in the presence of different concentrations of NO_2^-. Insert: Linear relationship between $(F_0\text{-}F)/F_0$ and the concentration of NO_2^- **(B)** Fluorescence recovery of the CDs with various SO_3^{2-} concentrations. Insert: Fitted line between $(F\text{-}F_0)/F$ and the concentration of SO_3^{2-}.

changed slightly by 5% under extreme acidic conditions, which may be due to a large number of hydroxyl groups on the surface of CDs. However, strong alkaline conditions can seriously affect the intensity of CDs. The NO_2^- and SO_3^{2-} detections in this work were all performed under natural conditions. Besides, the stability of the fluorescence intensity of CDs solution after storage for different time periods was also evaluated. The fluorescence intensity of the CDs solution decreased by only 13% during 6-days storage period, which indicate the good fluorescence stability of the CDs. And the relative quantum yield of CDs is 12.2% by using quinine sulfate as a reference. The robust fluorescence stability makes the CDs suitable for further bioimaging applications.

Fluorescence and Selectivity Response of CDs Toward NO_2^- and SO_3^{2-}

The "on-off-on" fluorescent probes based on CDs were developed to detect NO_2^- and SO_3^{2-}. As shown in **Figure 5A**, CDs have a specific binding ability with NO_2^- and the emission fluorescence intensity of CDs at 435 nm was gradually quenched along with the increasing concentration of NO_2^-. Also, the fluorescence intensity of CDs was quenched over 60% after adding of NO_2^- at the concentration of 400 μM, and then, the downward trend slows down with the NO_2^-. Furthermore, it is worth to point out that there was an excellent linear relationship ($R^2 = 0.999$) between the fluorescence ratio $(F_0\text{-}F)/F_0$ and the concentration of NO_2^-, where F_0 and F are the fluorescence intensities of the CDs in the absence and presence of NO_2^-. In addition, the limit detection of CDs for NO_2^- was 0.425 μM (LOD = 3σ/S, where σ is the standard deviation of the blank and s is the slope of the linear calibration plot). With the addition of SO_3^{2-}, the fluorescence intensity of CDs gradually recovered. As shown in **Figure 5B**, the emission intensities of this probe at 435 nm were recorded at 15 min after adding various concentration of SO_3^{2-}, which showed good linear relationship ($R^2 = 0.998$) between the fluorescence ratio $(F\text{-}F_0)/F_0$ and the concentration of NO_2^- in the range of 200–600 μM. The limit detection for SO_3^{2-} was determined to be 0.243 μM. The detection performance of CDs based "on-off-on" fluorescent sensor was comparable to previous reports (**Table 1**), articulating the availability and simplicity of the proposed sensing

TABLE 1 | Performance comparison of different fluorescence probes for the detection of SO_3^{2-} and NO_2^-

Materials	Ions detected	Limitation (μM)	Reference
Ammonium citrate (CDs)	SO_3^{2-}	0.35	Fang et al. (2017)
Gold nanoclusters	SO_3^{2-}	12	Sachdev et al. (2019)
NIR-SO2-TP	HSO_3^{2-}	1.06	Zhao et al. (2019c)
Corn	HSO_3^{2-}	0.5	Zhao et al. (2019a)
Fluorescein	SO_3^{2-}	1.74	Zhang et al. (2016)
Indole	SO_3^{2-}	0.57	Venkatachalam et al. (2020)
Ru-CHO	HSO_3^{2-}	0.52	Zhang et al. (2018)
Nicotinic acid, folic acid	NO_2^-	21.2	Gan et al. (2020)
Citric acid, phenylenediamine	NO_2^-	0.65	Jia et al. (2019)
Tris, urea	NO_2^-	13.5	Karali et al. (2018)
Sodium phytate, Na_2SO_4	NO_2^-	0.3	Wang et al. (2019b)
Starch	NO_2^-, SO_3^{2-}	0.425,0.243	This work

probe. Therefore, the results show that CDs can be considered as a good fluorescent probe for monitoring the concentration of NO_2^- and SO_3^{2-} with excellent sensitivity.

In order to evaluate the selectivity in sensing response of CDs, various metal ions (Cu^{2+}, Fe^{3+}, Ca^{2+}, K^+, Na^+), anions (NO_3^-, PO_4^{3-}, SO_4^{2-}, SO_3^{2-}) and organic molecules (Gly, GSH, Cys, Urea) were considered. **Figure 6A** displays the fluorescence intensities of CDs in the presence of NO_2^- as compared to multiple interfering ions. The fluorescence intensity was reduced by 90% by NO_2^- (500 μM). Therefore, CDs show desirable selectivity for the detection of NO_2^-. Although, Fe^{3+} affect the fluorescence intensity of CDs. Fortunately, the concentration of Fe^{3+} in plasma is low (**Supplementart Table 2**) and the false signals can be effectively shield by triethanolamine. Thus, CDs have potential for directive and selective detection of NO_2^- ions. Moreover, to evaluate the selectivity in sensing response of CDs to SO_3^{2-}, various metal ions (Ca^{2+}, K^+, Na^+), anions (SO_4^{2-}, HSO_3^{2-}) and organic molecules (Gly, GSH, Glu, Cys, Urea, Suc) were investigated for their impact on the fluorescence intensity of CDs/NO_2^-. As illustrated in **Figure 6B**, the fluorescent responses and the corresponding luminescence variations of organic molecules and metal ions was negligible compared to the presence of SO_3^{2-}. The degree of fluorescence intensity recovered by HSO_3^{2-} was equivalent to 57.8% fluorescence recovered by SO_3^{2-}. Therefore, the results confirmed that CDs had great potential for specifically detecting NO_2^- and SO_3^{2-}.

Mechanism of the Fluorescence Response of CDs to NO_2^- and SO_3^{2-}

To understand the fluorescence quenching mechanism of CDs, fluorescence lifetime decay, zeta potential, UV-vis absorption (**Supplementary Figure S2**) and electrochemical behaviors (**Supplementary Figure S3**) were investigated. After adding NO_2^- and SO_3^{2-}, signals of UV-vis absorption were almost unchanged and these results were consistent with observation in the cyclic voltammogram (CV) after adding NO_2^- and SO_3^{2-} (**Supplementary Figure S3**). The CV of CDs just showed a reversible redox reaction. Moreover, the fluorescence lifetimes were respectively 1.8 ns (CDs only), 2.03 ns (in the presence of NO_2^-) and 2.55 ns (in the presence of NO_2^- and SO_3^{2-}) in the **Supplementary Figure S4**, which displayed no obvious change and it is different from a dynamic fluorescence quenching mechanism, suggesting a static fluorescence quenching effect occurred. In detail, the zeta potential of CDs solution was

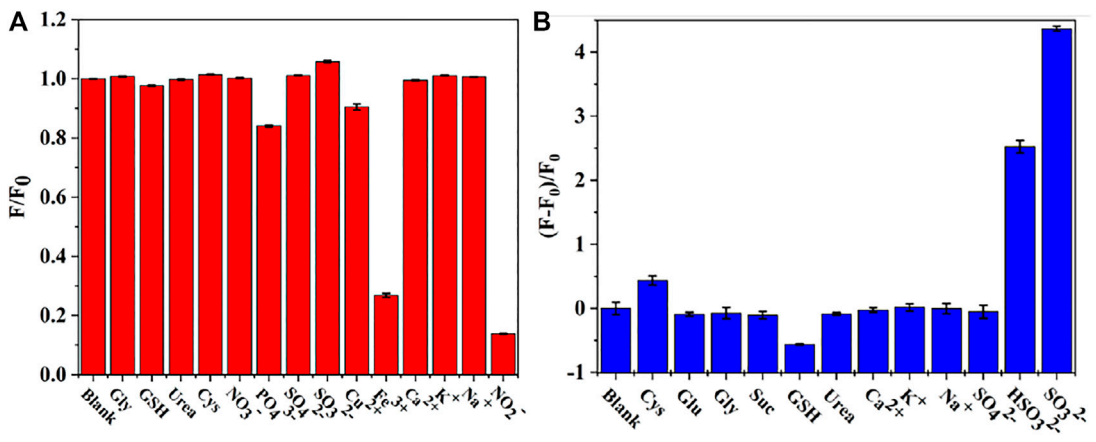

FIGURE 6 | (A) Selective test of the assay toward NO_2^- **(B)** Selectivity in the sensing response of CDs/NO_2^- toward SO_3^{2-}.

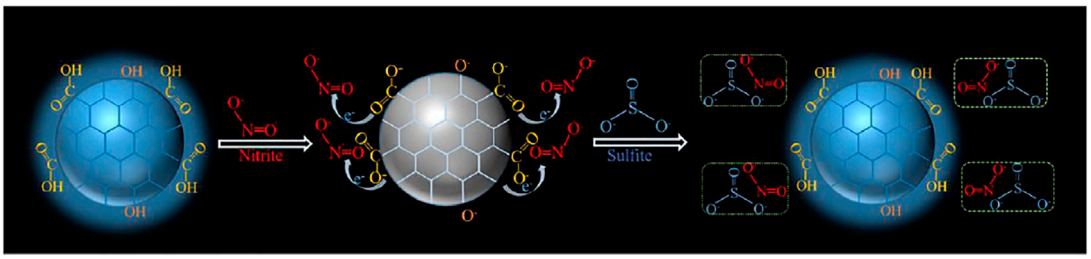

FIGURE 7 | Schematic diagram of CDs with NO_2^- and SO_3^{2-}.

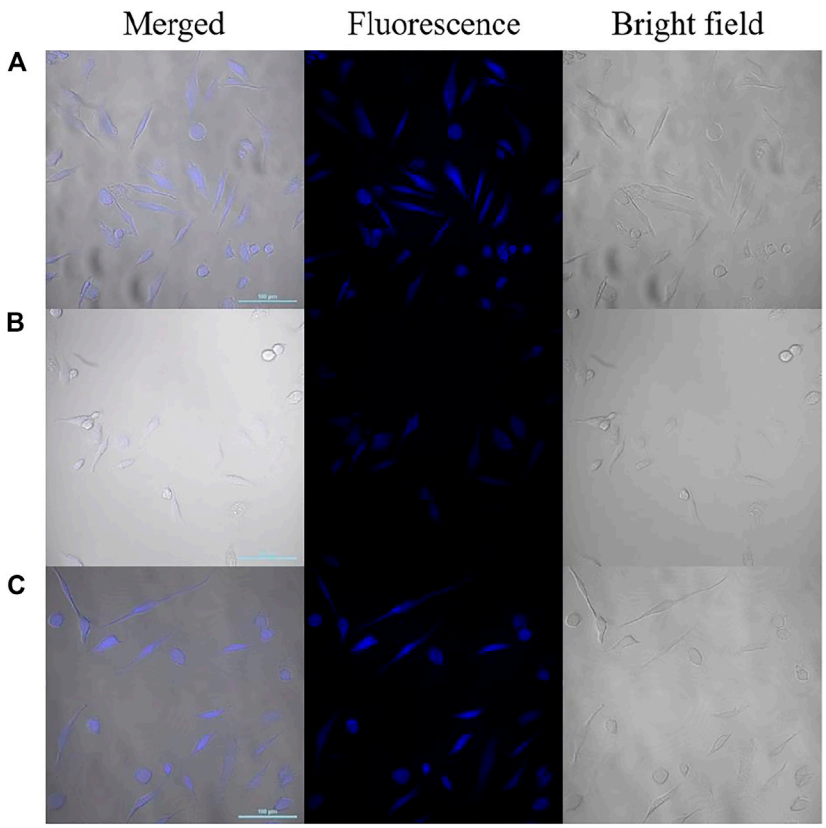

FIGURE 8 | Confocal laser fluorescence images of HeLa cells incubated with CDs **(A)**, CDs/NO_2^- **(B)** and CDs/NO_2^-/SO_3^{2-} **(C)** (Left: the merged image; middle: the fluorescence image; right: the bright field image; scale bar: 100 μm).

measured as -36.85 mV, which indicates that the nucleus of CDs is positively charged and the surface is rich in anions. After the introduction of NO_2^-, it replaces the anions on the surface of CDs. And the strong electron absorption of NO_2^- makes it difficult for the electrons in the CDs core to be excited, leading to fluorescence quenching. When SO_3^{2-} was introduced, SO_3^{2-} would reduce NO_2^- and destroy the charge transfer between NO_2^- and CDs, resulting in fluorescence recovery (**Figure 7**).

Cytotoxicity Test and Intracellular Sensing

Before imaging, the cytotoxicity of CDs to HeLa cells was assessed using WST assay. Various concentrations of CDs (20, 50, 100, 200, 300, 400, 500 μg ml^{-1}) were added to Hela cells and cell viability was observed more than 90% after incubating HeLa cells with CDs for 24 h (**Supplementary Figure S4**). Owing to their low cytotoxicity and excellent biocompatibility, the fluorescent probe was used to image NO_2^- and SO_3^{2-} in live cells.

The possibility of CDs to be as a label agent for fluorescent bioimaging of $NO_2^-$and SO_3^{2-} was tested by a confocal laser microscopy. As shown in **Figure 8**, Hela cells treated with CDs solution (200 μg ml^{-1}) exhibit blue fluorescence and retained normal morphology. Upon incubation with NO_2^- for 20 min, the fluorescence in the living cells was significantly quenched. After adding SO_3^{2-}, the fluorescence recovered effectively. These

results are consistent with the observed results in spectral experiments, which suggest that the fluorescent probe have the potential to detect NO_2^- and SO_3^{2-} in living cells.

CONCLUSION

In summary, we have developed a highly sensitive and selective fluorescence probe for the detection nitrite ions and sulfite ions. The fluorescence of CDs was efficiently quenched by nitrite ions through a static quench mechanism, which was confirmed by the fluorescence lifetime. Because of the specific reactive response of CDs to nitrite ions and sulfite ions, the fluorescence of "on-off-on" sensor was quenched via nitrite ions and the weak fluorescence was enhanced upon addition of sulfite ions. Thus, the fluorescent probe can be used to detect nitrite ions and sulfite ions with convenience, high sensitivity and selectivity. Owing to low cytotoxicity and good biocompatibility, CDs have been used to image NO_2^- and SO_3^{2-} in HeLa cell. Therefore, this method may provide a new route for sensing nitrite and sulfite derivatives in environment and living cells.

DATA AVAILABILITY STATEMENT

The original contributions presented in the study are included in the article/**Supplementary Material**, further inquiries can be directed to the corresponding authors.

AUTHOR CONTRIBUTIONS

PW: Conceptualization, Methodology, Writing - original draft. LI: Software, Data curation, Writing - review and editing. YL: Methodology, Data curation. XP: Methodology, Data curation. PL: Methodology, Data curation. YZ: Methodology, Data curation. W-FD: Methodology, Data curation, Validation. RY: Supervision, Software, Validation, Writing - review and editing.

FUNDING

This research was funded by the National Key R&D Program of China (No. 2020YFC2004600), the National Natural Science Foundation of China (No. 21803075), the Primary Research and Development Plan of Jiangsu Province (No. BE2019683), the Science Foundation of the Chinese Academy of Sciences (No. 2020SYHZ0041), the Science and Technology Department of Jinan City (No. 2018GXRC016) and the Instrument Developing Project of Chinese Academy of Science (YJKYYQ20200038).

SUPPLEMENTARY MATERIAL

The Supplementary Material for this article can be found online at: https://www.frontiersin.org/articles/10.3389/fchem.2021.782238/full#supplementary-material

REFERENCES

Asaithambi, G., and Periasamy, V. (2020). Ratiometric Sensing of Sulfite/bisulfite Ions and its Applications in Food Samples and Living Cells. *J. Photochem. Photobiol. A: Chem.* 389, 112214. doi:10.1016/j.jphotochem.2019.112214

Boningari, T., and Smirniotis, P. G. (2016). Impact of Nitrogen Oxides on the Environment and Human Health: Mn-Based Materials for the NO x Abatement. *Curr. Opin. Chem. Eng.* 13, 133–141. doi:10.1016/j.coche.2016.09.004

Cockburn, A., Brambilla, G., Fernández, M.-L., Arcella, D., Bordajandi, L. R., Cottrill, B., et al. (2013). Nitrite in Feed: from Animal Health to Human Health. *Toxicol. Appl. Pharmacol.* 270 (3), 209–217. doi:10.1016/j.taap.2010.11.008

Della Betta, F., Vitali, L., Fett, R., and Costa, A. C. O. (2014). Development and Validation of a Sub-minute Capillary Zone Electrophoresis Method for Determination of Nitrate and Nitrite in Baby Foods. *Talanta* 122, 23–29. doi:10.1016/j.talanta.2014.01.006

Fang, L., Zhang, L., Chen, Z., Zhu, C., Liu, J., and Zheng, J. (2017). Ammonium Citrate Derived Carbon Quantum Dot as On-Off-On Fluorescent Sensor for Detection of Chromium(VI) and Sulfites. *Mater. Lett.* 191, 1–4. doi:10.1016/j.matlet.2016.12.098

Forman, D., Al-Dabbagh, S., and Doll, R. (1985). Nitrate and Gastric Cancer Risks. *Nature* 317 (6039), 676. doi:10.1038/317676a0

Furman, S., Lichtstein, D., and Ilani, A. (1997). Sodium-dependent Transport of Phosphate in Neuronal and Related Cells. *Biochim. Biophys. Acta Biomembr.* 1325 (1), 34–40. doi:10.1016/s0005-2736(96)00238-6

Gan, L., Su, Q., Chen, Z., and Yang, X. (2020). Exploration of pH-Responsive Carbon Dots for Detecting Nitrite and Ascorbic Acid. *Appl. Surf. Sci.* 530, 147269. doi:10.1016/j.apsusc.2020.147269

Ge, J., Jia, Q., Liu, W., Guo, L., Liu, Q., Lan, M., et al. (2015). Red-Emissive Carbon Dots for Fluorescent, Photoacoustic, and Thermal Theranostics in Living Mice. *Adv. Mater.* 27 (28), 4169–4177. doi:10.1002/adma.201500323

Grabolle, M., Spieles, M., Lesnyak, V., Gaponik, N., Eychmüller, A., and Resch-Genger, U. (2009). Determination of the Fluorescence Quantum Yield of Quantum Dots: Suitable Procedures and Achievable Uncertainties. *Anal. Chem.* 81 (15), 6285–6294. doi:10.1021/ac900308v

Gu, Z., Wu, M.-L., Yan, B.-Y., Wang, H.-F., and Kong, C. (2020). Integrated Digital Microfluidic Platform for Colorimetric Sensing of Nitrite. *ACS Omega* 5 (19), 11196–11201. doi:10.1021/acsomega.0c01274

Heaviside, C., Witham, C., and Vardoulakis, S. (2021). Potential Health Impacts from sulphur Dioxide and Sulphate Exposure in the UK Resulting from an Icelandic Effusive Volcanic Eruption. *Sci. Total Environ.* 774, 145549. doi:10.1016/j.scitotenv.2021.145549

Iammarino, M., Di Taranto, A., Muscarella, M., Nardiello, D., Palermo, C., and Centonze, D. (2010). Development of a New Analytical Method for the Determination of Sulfites in Fresh Meats and Shrimps by Ion-Exchange Chromatography with Conductivity Detection. *Analyt. Chim. Acta* 672 (1-2), 61–65. doi:10.1016/j.aca.2010.04.002

Jia, J., Lu, W.-J., Li, L., Jiao, Y., Gao, Y.-F., and Shuang, S.-M. (2019). Orange Luminescent Carbon Dots as Fluorescent Probe for Detection of Nitrite. *Chin. J. Anal. Chem.* 47 (4), 560–566. doi:10.1016/s1872-2040(19)61155-2

Jiang, Y. J., Lin, M., Yang, T., Li, R. S., Huang, C. Z., Wang, J., et al. (2019). Nitrogen and Phosphorus Doped Polymer Carbon Dots as a Sensitive Cellular Mapping Probe of Nitrite. *J. Mater. Chem. B* 7 (12), 2074–2080. doi:10.1039/c8tb02998a

Jiao, Y., Gao, Y., Meng, Y., Lu, W., Liu, Y., Han, H., et al. (2019). One-Step Synthesis of Label-free Ratiometric Fluorescence Carbon Dots for the Detection of Silver Ions and Glutathione and Cellular Imaging Applications. *ACS Appl. Mater. Inter.* 11 (18), 16822–16829. doi:10.1021/acsami.9b01319

Jin, J., Li, L., Zhang, L., Luan, Z., Xin, S., and Song, K. (2021). Progress in the Application of Carbon Dots-Based Nanozymes. *Front. Chem.* 9, 748044. doi:10.3389/fchem.2021.748044

Joseph, E. P., Beckles, D. M., Cox, L., Jackson, V. B., and Alexander, D. (2015). An Evaluation of Ambient sulphur Dioxide Concentrations from Passive Degassing of the Sulphur Springs, Saint Lucia Geothermal System:

Implications for Human Health. *J. Volcanol. Geotherm. Res.* 304, 38–48. doi:10.1016/j.jvolgeores.2015.07.036

Kalaycıoğlu, Z., and Erim, F. B. (2019). Nitrate and Nitrites in Foods: Worldwide Regional Distribution in View of Their Risks and Benefits. *J. Agric. Food Chem.* 67 (26), 7205–7222. doi:10.1021/acs.jafc.9b01194

Karali, K. K., Sygellou, L., and Stalikas, C. D. (2018). Highly Fluorescent N-Doped Carbon Nanodots as an Effective Multi-Probe Quenching System for the Determination of Nitrite, Nitrate and Ferric Ions in Food Matrices. *Talanta* 189, 480–488. doi:10.1016/j.talanta.2018.07.008

Khan, M., and Lively, J. A. (2020). Determination of Sulfite and Antimicrobial Residue in Imported Shrimp to the USA. *Aquac. Rep.* 18, 100529. doi:10.1016/j.aqrep.2020.100529

Langer, M., Paloncýová, M., Medveď, M., Pykal, M., Nachtigallová, D., Shi, B., et al. (2021). Progress and Challenges in Understanding of Photoluminescence Properties of Carbon Dots Based on Theoretical Computations. *Appl. Mater. Today* 22, 100924. doi:10.1016/j.apmt.2020.100924

Li, S., Guo, Z., Zhang, Y., Xue, W., and Liu, Z. (2015). Blood Compatibility Evaluations of Fluorescent Carbon Dots. *ACS Appl. Mater. Inter.* 7 (34), 19153–19162. doi:10.1021/acsami.5b04866

Li, Y.-S., Zhao, C.-L., Li, B.-L., and Gao, X.-F. (2020). Evaluating Nitrite Content Changes in Some Chinese home Cooking with a Newely-Developed CDs Diazotization Spectrophotometry. *Food Chem.* 330, 127151. doi:10.1016/j.foodchem.2020.127151

Lundberg, J. O., Weitzberg, E., and Gladwin, M. T. (2008). The Nitrate-Nitrite-Nitric Oxide Pathway in Physiology and Therapeutics. *Nat. Rev. Drug Discov.* 7 (2), 156–167. doi:10.1038/nrd2466

Mojić, M., Pristov, J. B., Maksimović-Ivanić, D., Jones, D. R., Stanić, M., Mijatović, S., et al. (2014). Extracellular Iron Diminishes Anticancer Effects of Vitamin C: an *In Vitro* Study. *Sci. Rep.* 4, 5955. doi:10.1038/srep05955

Nazri, N. A. A., Azeman, N. H., Luo, Y., and A Bakar, A. A. (2021). Carbon Quantum Dots for Optical Sensor Applications: A Review. *Opt. Laser Techn.* 139, 106928. doi:10.1016/j.optlastec.2021.106928

Olmsted, J. (1979). Calorimetric Determinations of Absolute Fluorescence Quantum Yields. *J. Phys. Chem.* 83 (20), 2581–2584. doi:10.1021/j100483a006

Pan, X. (2019). "Sulfur Oxides," in *Encyclopedia of Environmental Health*. Oxford, United Kingdom: Elsevier, 823–829. doi:10.1016/b978-0-12-409548-9.11333-8

Park, S.-H., Hwang, I., McNaughton, D. A., Kinross, A. J., Howe, E. N. W., He, Q., et al. (2021). Synthetic Na+/K+ Exchangers Promote Apoptosis by Disturbing Cellular Cation Homeostasis. *Chem*. doi:10.1016/j.chempr.2021.08.018

Qu, Z., Liu, L., Sun, T., Hou, J., Sun, Y., Yu, M., et al. (2020). Synthesis of Bifunctional Carbon Quantum Dots for Bioimaging and Anti-inflammation. *Nanotechnology* 31 (17), 175102. doi:10.1088/1361-6528/ab6b9d

Sachdev, A., Raj, R., Matai, I., Kumar, V., Gopinath, P., and Mishra, S. (2019). Label-free Fluorescence "Turn-On" Detection of SO32− by Gold Nanoclusters: Integration in a Hydrogel Platform and Intracellular Detection. *Anal. Methods* 11 (9), 1214–1223. doi:10.1039/c8ay02813c

Sun, Y.-P., Zhou, B., Lin, Y., Wang, W., Fernando, K. A. S., Pathak, P., et al. (2006). Quantum-sized Carbon Dots for Bright and Colorful Photoluminescence. *J. Am. Chem. Soc.* 128 (24), 7756–7757. doi:10.1021/ja062677d

Tang, S., Wong, H.-C., Wang, Z.-M., Huang, Y., Zou, J., Zhuo, Y., et al. (2011). Design and Application of a Class of Sensors to Monitor Ca2+ Dynamics in High Ca2+ Concentration Cellular Compartments. *Proc. Natl. Acad. Sci.* 108 (39), 16265–16270. doi:10.1073/pnas.1103015108

Tapiero, H., Townsend, D. M., and Tew, K. D. (2003). Trace Elements in Human Physiology and Pathology. Copper. *Biomed. Pharmacother.* 57 (9), 386–398. doi:10.1016/s0753-3322(03)00012-x

Tosic, J., Stanojevic, Z., Vidicevic, S., Isakovic, A., Ciric, D., Martinovic, T., et al. (2019). Graphene Quantum Dots Inhibit T Cell-Mediated Neuroinflammation in Rats. *Neuropharmacology* 146, 95–108. doi:10.1016/j.neuropharm.2018.11.030

Venkatachalam, K., Asaithambi, G., Rajasekaran, D., and Periasamy, V. (2020). A Novel Ratiometric Fluorescent Probe for "Naked-Eye" Detection of Sulfite Ion: Applications in Detection of Biological SO32− Ions in Food and Live Cells. *Spectrochim. Acta A: Mol. Biomol. Spectrosc.* 228, 117788. doi:10.1016/j.saa.2019.117788

Wang, R., Wang, R., Ju, D., Lu, W., Jiang, C., Shan, X., et al. (2018a). "ON-OFF-ON" Fluorescent Probes Based on Nitrogen-Doped Carbon Dots for Hypochlorite and Bisulfite Detection in Living Cells. *Analyst* 143 (23), 5834–5840. doi:10.1039/c8an01585f

Wang, S., Cao, X., Gao, T., Wang, X., Zou, H., and Zeng, W. (2018b). A Ratiometric Upconversion Nanoprobe for Fluorometric Turn-On Detection of Sulfite and Bisulfite. *Microchim Acta* 185 (4), 218. doi:10.1007/s00604-018-2757-y

Wang, J., Zhu, Y., and Wang, L. (2019a). Synthesis and Applications of Red-Emissive Carbon Dots. *Chem. Rec.* 19 (10), 2083–2094. doi:10.1002/tcr.201800172

Wang, W., Xu, S., Li, N., Huang, Z., Su, B., and Chen, X. (2019b). Sulfur and Phosphorus Co-doped Graphene Quantum Dots for Fluorescent Monitoring of Nitrite in Pickles. *Spectrochim. Acta Part A: Mol. Biomol. Spectrosc.* 221, 117211. doi:10.1016/j.saa.2019.117211

Wang, P., Li, L., Pang, X., Zhang, Y., Zhang, Y., Dong, W.-F., et al. (2021a). Chitosan-based Carbon Nanoparticles as a Heavy Metal Indicator and for Wastewater Treatment. *RSC Adv.* 11 (20), 12015–12021. doi:10.1039/d1ra00692d

Wang, P., Sun, Y., Li, X., Shan, J., Xu, Y., and Li, G. (2021b). One-step Chemical Reaction Triggered Surface Enhanced Raman Scattering Signal Conversion Strategy for Highly Sensitive Detection of Nitrite. *Vib. Spectrosc.* 113, 103221. doi:10.1016/j.vibspec.2021.103221

Wang, Y., Lei, L., Liu, E., Cheng, Y., and Xu, S. (2021c). Constructing Highly Sensitive Ratiometric Nanothermometers Based on Indirectly Thermally Coupled Levels. *Chem. Commun.* 57 (72), 9092–9095. doi:10.1039/d1cc03407c

Wang, Y., Lei, L., Ye, R., Jia, G., Hua, Y., Deng, D., et al. (2021d). Integrating Positive and Negative Thermal Quenching Effect for Ultrasensitive Ratiometric Temperature Sensing and Anti-counterfeiting. *ACS Appl. Mater. Inter.* 13 (20), 23951–23959. doi:10.1021/acsami.1c05611

Würth, C., Grabolle, M., Pauli, J., Spieles, M., and Resch-Genger, U. (2013). Relative and Absolute Determination of Fluorescence Quantum Yields of Transparent Samples. *Nat. Protoc.* 8 (8), 1535–1550. doi:10.1038/nprot.2013.087

Yarur, F., Macairan, J.-R., and Naccache, R. (2019). Ratiometric Detection of Heavy Metal Ions Using Fluorescent Carbon Dots. *Environ. Sci. Nano* 6 (4), 1121–1130. doi:10.1039/c8en01418c

Yue, J., Li, L., Cao, L., Zan, M., Yang, D., Wang, Z., et al. (2019). Two-Step Hydrothermal Preparation of Carbon Dots for Calcium Ion Detection. *ACS Appl. Mater. Inter.* 11 (47), 44566–44572. doi:10.1021/acsami.9b13737

Zan, M., Li, C., Liao, F., Rao, L., Meng, Q.-F., Xie, W., et al. (2020). One-step Synthesis of green Emission Carbon Dots for Selective and Sensitive Detection of Nitrite Ions and Cellular Imaging Application. *RSC Adv.* 10 (17), 10067–10075. doi:10.1039/c9ra11009g

Zhang, J. B., Zhang, H., Wang, H. L., Zhang, J. Y., Luo, P. J., Zhu, L., et al. (2014). Risk Analysis of Sulfites Used as Food Additives in China. *Biomed. Environ. Sci.* 27 (2), 147–154. doi:10.3967/bes2014.032

Zhang, Y., Shao, X., Wang, Y., Pan, F., Kang, R., Peng, F., et al. (2015). Dual Emission Channels for Sensitive Discrimination of Cys/Hcy and GSH in Plasma and Cells. *Chem. Commun.* 51 (20), 4245–4248. doi:10.1039/c4cc08687b

Zhang, H., Xue, S., and Feng, G. (2016). A Colorimetric and Near-Infrared Fluorescent Turn-On Probe for Rapid Detection of Sulfite. *Sensors Actuators B: Chem.* 231, 752–758. doi:10.1016/j.snb.2016.03.069

Zhang, W., Liu, H., Zhang, F., Wang, Y.-L., Song, B., Zhang, R., et al. (2018). Development of a Ruthenium(II) Complex-Based Luminescence Probe for Detection of Hydrogen Sulfite in Food Samples. *Microchem. J.* 141, 181–187. doi:10.1016/j.microc.2018.05.031

Zhang, Y., Zhou, K., Qiu, Y., Xia, L., Xia, Z., Zhang, K., et al. (2021). Strongly Emissive Formamide-Derived N-Doped Carbon Dots Embedded Eu(III)-based Metal-Organic Frameworks as a Ratiometric Fluorescent Probe for Ultrasensitive and Visual Quantitative Detection of Ag+. *Sensors Actuators B: Chem.* 339, 129922. doi:10.1016/j.snb.2021.129922

Zhao, J., Peng, Y., Yang, K., Chen, Y., Zhao, S., and Liu, Y.-M. (2019a). A New Ratiometric Fluorescence Assay Based on Resonance Energy Transfer between Biomass Quantum Dots and Organic Dye for the Detection of Sulfur Dioxide Derivatives. *RSC Adv.* 9 (71), 41955–41961. doi:10.1039/c9ra09437g

Zhao, W., Yang, H., Xu, S., Li, X., Wei, W., and Liu, X. (2019b). "Olive-Structured" Nanocomposite Based on Multiwalled Carbon Nanotubes Decorated with an Electroactive Copolymer for Environmental Nitrite

Detection. *ACS Sustain. Chem. Eng.* 7 (20), 17424–17431. doi:10.1021/acssuschemeng.9b04616

Zhao, Y., Ma, Y., and Lin, W. (2019c). A Near-Infrared and Two-Photon Ratiometric Fluorescent Probe with a Large Stokes Shift for Sulfur Dioxide Derivatives Detection and its Applications *In Vitro* and *In Vivo*. *Sensors Actuators B: Chem.* 288, 519–526. doi:10.1016/j.snb.2019.01.170

Zhi, B., Cui, Y., Wang, S., Frank, B. P., Williams, D. N., Brown, R. P., et al. (2018). Malic Acid Carbon Dots: From Super-resolution Live-Cell Imaging to Highly Efficient Separation. *ACS Nano* 12 (6), 5741–5752. doi:10.1021/acsnano.8b01619

Zuo, Y., and Chen, H. (2003). Simultaneous Determination of Sulfite, Sulfate, and Hydroxymethanesulfonate in Atmospheric Waters by Ion-Pair HPLC Technique. *Talanta* 59 (5), 875–881. doi:10.1016/s0039-9140(02)00647-1

Conflict of Interest: W-FD and QM was employed by the company Jinan Guokeyigong Science and Technology Development Co., Ltd.

The remaining authors declare that the research was conducted in the absence of any commercial or financial relationships that could be construed as a potential conflict of interest.

Publisher's Note: All claims expressed in this article are solely those of the authors and do not necessarily represent those of their affiliated organizations, or those of the publisher, the editors and the reviewers. Any product that may be evaluated in this article, or claim that may be made by its manufacturer, is not guaranteed or endorsed by the publisher.